TRANSIENT DUTY CYCLE ANALYSIS FOR MOBILE ORGANIC RANKINE CYCLE APPLICATIONS

Miles C Robertson[†], Aaron W Costall*, Peter J Newton and Ricardo F Martinez-Botas

[*]*Corresponding Author*, [†]*Presenting Author*

Department of Mechanical Engineering,
Imperial College London
City & Guilds Building
South Kensington Campus
London SW7 2AZ, UK
email: a.costall@imperial.ac.uk

ABSTRACT

Internal combustion engines have high exhaust energy at the tail pipe, and mobile organic Rankine cycle (ORC) systems have been proposed to harness this waste heat, thereby providing a significant opportunity for vehicle CO_2 emissions reduction. This paper discusses the impact of transient duty cycles on mobile ORC system performance. A thermodynamic model of an ORC system is presented, which includes a detailed heat exchanger model based on the Effectiveness-NTU method, and which has the ability to account for the thermal capacitance of the ORC system – which is of particular importance during vehicle start-up. Thermodynamic system simulations from start-up were performed based on four transient engine test cycles applied to a simulated 11.7L heavy-duty diesel engine: the Constant-Speed, Variable-Load (CSVL) cycle, the European Transient Cycle (ETC), the Non-Road Transient Cycle (NRTC), and the World Harmonized Transient Cycle (WHTC). For a fixed heat exchanger size, working fluid and ORC mass flow rate, it was found that the relatively high-load CSVL cycle (acting as a surrogate for an off-road machine) produced a peak average power of 9.0 kW from start-up, while the WHTC (representative of on-highway driving conditions) only delivered 3.2 kW. Results also indicate a very narrow band (5.5–6.2%) of peak exhaust energy recovery across all duty cycles, implying a close to linear scaling of ORC system power output with duty cycle intensity and engine size. The choice of vehicle/application is thus constrained by the ability to design an acceptable low-power ORC expander, suggesting that vehicles running the most heavily-loaded duty cycles stand to gain the most benefit from mobile ORC systems.

1. INTRODUCTION

Worldwide concern for lowering transport-related CO_2 emissions is driving internal combustion (IC) engine manufacturers to investigate new powertrain technologies. For example, the first fuel economy standards for US heavy-duty vehicles were announced in 2011 for years 2014–2018, with the largest trucks set a 20% target reduction by the end of that period (EPA, 2011). Unlike passenger car engines, heavy-duty diesel engines in commercial vehicle and off-road sectors are not well-suited for full electrification. Reduction of CO_2 emissions from these applications will continue to require improvements in conventional IC engine powertrains (Auto Council, 2011). Waste heat rejected to the exhaust is a significant portion of the fuel energy (Howey *et al*., 2010), depending on the particular engine operating point, and waste heat recovery (WHR) technologies offer system efficiency enhancements in the near term (Greszler, 2012). Once the available high pressure and temperature energy is extracted (by turbocharging and, if present, turbocompounding), part of the remaining lower grade exhaust energy may be recovered via a bottoming cycle, such as the organic Rankine cycle.

ORC plants have been used for stationary power generation since the 1960s (Uusitalo *et al*., 2011), taking advantage of biomass, geothermal, solar and numerous other heat energy sources. The benefits

of ORC applied to WHR in IC engines have been considered at various times since the late 1970s (Leising *et al*., 1978; Aly, 1988; Endo *et al.*, 2007; Katsanos *et al.*, 2012) and more recently in the form of a Rankine (i.e., steam) cycle for a BMW turbocharged gasoline passenger car engine (Horst *et al.*, 2014). The heat rejected to the coolant and the exhaust system are the two common sources (some systems also utilize the EGR loop), and are typically categorized as low- and medium-grade, respectively (Sprouse and Depcik, 2013). This technology has been shown to deliver up to 13% improvement to fuel economy (DiNanno *et al*., 1983). A recent large industrial research effort has sought to develop an ORC system for on-highway trucks under the US DOE SuperTruck program. This ORC WHR system contributed to the achievement of a brake thermal efficiency greater than 50% (Koeberlein, 2013). Nevertheless, duty cycles for on-highway trucks, city buses, various other commercial vehicles, and the vast number of off-highway machine applications are very diverse. In this work a thermodynamic system simulation is developed and applied transiently using reference duty cycle inputs from a selection of test cycles for heavy-duty engine applications. The purpose of this paper is to compare the influence of different duty cycles on mobile ORC system performance.

2. METHODOLOGY

2.1. System Level Overview

A basic schematic of the simulated ORC system is shown in Figure 1.

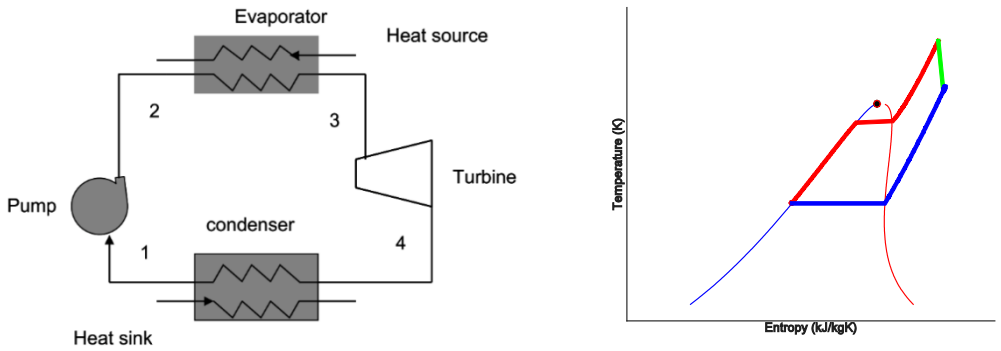

Figure 1: Basic block schematic of the ORC system (left) and corresponding T-S diagram (right)

The core layout consists of the fundamental Rankine cycle components – pump, evaporator, expander and condenser. A recuperator has been omitted from the design, due to the cost, weight and packaging penalties which make it unattractive for a mobile application. Although a recuperator increases cycle efficiency, this is of secondary importance to the ORC output power (Quoilin *et al.*, 2010).

2.2. Heat Exchanger Modeling

The focus of the current work is the accurate characterization of the transient heat flow between the vehicle exhaust flow and the ORC working fluid. A methodology was therefore developed which allowed modeling of the thermal capacitance of both fluid streams, along with the intermediate heat exchanger elements. The heat exchanger was modeled as a once-through/single pass design, consisting of an inner exhaust pipe enclosed by a concentric annular section containing the ORC working fluid. This design allows preheating, boiling and superheating of the working fluid within a single pipe. This avoids the requirement to hold excess fluid within a boiler drum, and the addition of unnecessary weight, which is to be discouraged in mobile applications (Quoilin *et al.*, 2013).

Considering practical aspects of ORC design, the Effectiveness-NTU method was chosen to allow compatibility with real-world evaporator design, along with the majority of heat transfer literature (e.g., Incropera *et al.*, 2006). By assuming quasi-steady behavior, a prediction of steady-state thermodynamic values can be generated, given the conditions at the current time step. An exponential relationship could therefore be defined, linking the temperature at the current time step, $T(t)$ to its infinite, steady-state solution, T_{inf}. This is shown in Equation (1), where the time constant $\tau(t)$ is an

unknown, defined from the thermodynamic conditions within the heat exchanger (Lachi *et al.*, 1997). An exponential projection of the temperature profile between the current time step and steady-state could therefore be drawn, before being truncated at the subsequent time step to provide an estimate of the transient temperature profile up to this point.

$$\frac{T(t)-T_{\mathrm{inf}}}{T_0-T_{\mathrm{inf}}} = e^{-t/\tau(t)} \tag{1}$$

Definition of the fluid time constant, τ, requires knowledge of the heat exchanger thermal capacitance. This is defined as the sum of the individual heat capacities of the exhaust gas, the ORC working fluid, and the heat exchanger pipe and casing metal (C_{exh}, C_{orc}, C_{pipe}, and C_{casing}, resp.), as in Equation (2) (Lachi *et al.*, 1997). Metal capacitances are constant, but fluid capacitances are time-varying, with temperature effects manifested in changes to specific heat capacity and density (altering the fluid mass contained in the heat exchanger, local fluid velocity and heat transfer correlations).

$$C(t) = C_{\mathrm{exh}}(t) + C_{\mathrm{orc}}(t) + C_{\mathrm{pipe}} + C_{\mathrm{casing}} \tag{2}$$

Fluid in the evaporator will be composed of different proportions of sub-cooled, boiling and superheated states, which are variable along the heat exchanger length. For example, a sub-cooled outlet state means wholly sub-cooled flow along the entire length of the heat exchanger; a boiling outlet implies portions of sub-cooled and boiling flow; while a superheated outlet requires all three phases within the heat exchanger. To accurately simulate the multi-phase phenomena within the heat exchanger, the three processes (sub-cooled, boiling and super-heated) were modeled separately, each with its own set of heat transfer coefficients and effectiveness relationships. The contribution from each process was determined iteratively from the ORC outlet enthalpy, with convergence achieved following successive calculations of a reference temperature (taken as the mean of the inlet and outlet values) to within a tolerance of 0.1°C. Single-phase flow was modeled using the Gnielinski forced heat transfer correlation (Incropera *et al.*, 2006) in Equation (5), where f is the wall friction factor. Two-phase ORC flow was modeled using the Gungor-Winterton boiling correlation (Gungor and Winterton, 1986) shown in Equation (6), where h_{TP}, h_{l}, and h_{pool} are respectively the heat transfer coefficients for two-phase, liquid and pool boiling, E is the enhancement factor, and S the suppression factor. Both models were validated against existing data prior to insertion in the model (Kakaç, 1991).

$$Nu_{\mathrm{D}} = \frac{(f/8)(Re_{\mathrm{D}}-1000)Pr}{1+12.7(f/8)^{1/2}\left(Pr^{2/3}-1\right)} \tag{5}$$

$$h_{\mathrm{TP}} = Eh_{\mathrm{l}} + Sh_{\mathrm{pool}} \tag{6}$$

2.3. Cycle Specification and Heat Exchanger Sizing

The primary aspects of the ORC cycle simulation are listed in Table 1. A pressure ratio of 15 was chosen as a realistic value for a radial turbine expander. The low pressure level (160 kPa) assumes condensing to an ambient temperature of 300 K, maintaining a positive gauge pressure to avoid air ingress into the condenser (Badr *et al.*, 1985). Combined with the pressure ratio, this fixes the high pressure level at 2400 kPa. The heat exchanger volume is a key parameter, directly influencing working fluid velocity and its subsequent impact upon heat transfer and thermal capacitance correlations. Furthermore, it will be a significant contributor to overall mobile ORC system volume, which will be limited by packaging constraints. To investigate the effect of heat exchanger sizing on cycle transient characteristics, three sets of heat exchanger dimensions were used (Table 2). Designs **HE1** and **HE2** investigate differences caused by changing the volume of ORC fluid contained within the heat exchanger. **HE3** increases the volume of metal components and its thermal capacitance.

2.4. ORC Expander Modeling and Work Output

The selection of a radial turbine as the ORC expander was assumed in this work, and in order to include the effect of turbine size on overall cycle performance, an efficiency map based approach was used. The values of turbine efficiency in the map are dependent upon variations in density ratio and

size parameter, assuming operation at the optimum specific speed (Macchi and Perdichizzi, 1981). This method is useful since it does not assume constant turbine efficiency, but is much less complex than incorporating a full meanline model (e.g., Costall *et al.*, 2015).

Table 1: Summary of key cycle parameters

Parameter	Value
Working fluid	R245fa
Maximum temperature (°C)	300
High cycle pressure (kPa)	2400
Low cycle pressure (kPa)	160
Turbine pressure ratio (-)	15
Ambient (start-up) temperature (°C)	15

Table 2: Heat exchanger sizing combinations

	Exhaust Outer Dia. (mm)	Tube Thickness (mm)	ORC Outer Dia. (mm)	Casing Thickness (mm)	Description
HE1	70	6	96	6	Large ORC volume
HE2	70	6	86	6	Small ORC volume
HE3	70	12	92	12	Increased metal volume

2.5. Operating Logic Structure

In order to model the effects of vehicle start-up, several different modes of operation must be defined. These are shown schematically in Figure 2, and described here:

(a) Warm-up occurs exclusively at the start of each simulation. The ORC fluid is assumed to begin at the ambient temperature (modeled as -10°C) – if this is below the condenser set-point temperature then the fluid is circulated round the evaporator and condenser at the minimum cycle pressure, until the condenser outlet set-point has been established.

(b) Sub-cooled conditions at the heat exchanger outlet mean that no work can be extracted from the turbine. The most efficient path to boiling is therefore to circulate fluid around the heat exchanger to begin generating vapor. At this point the evaporator pressure is raised to its 'high' value (2400 kPa), assuming perfect pump pressure regulation.

(c) Boiling conditions at heat exchanger outlet result in a mixture of vapor and steam – these are divided in the separator. Fluid is recirculated to raise evaporator inlet enthalpy, whilst vapor passes through the turbine and condenser, facilitating approximation of part-load operation.

(d) Super-heated conditions at the heat exchanger outlet allow the entire ORC flow to be passed through the turbine and condenser – the other paths are closed off.

Optimal control of these modes is not attempted in the current work, though it is a major challenge for ORC applications, and examples of optimization tools are available (e.g., Peralez *et al.*, 2014).

2.6. Duty Cycle Data

A separate cycle simulation of an 11.7L Scania DC12 Euro 3 diesel engine validated against dynamometer test data (Hedbom, 2007) was used to generate maps of exhaust mass flow rate and temperature, at 89 full- and part-load operating points, between engine speeds of 600 and 2350 rpm. The transient thermodynamic ORC model interpolated this dataset at every instance in the four duty cycles listed in Table 3, obtaining the time-varying evaporator heat input powers shown in Figure 3.

3. RESULTS

3.1. Initial Transient Model Results

The time-varying exhaust conditions (generated in GT-POWER from duty cycle speed/load data) were used as an input to the transient thermodynamic ORC model, to generate cycle performance

predictions. Figure 4 shows how the proportion of sub-cooled, boiling and super-heated flow at the heat exhanger exit varies across a single WHTC duty cycle. Due to the once-through/single pass design, even when the heat exchanger outlet is super-heated, sub-cooled and boiling effects often dominate the entire heat exchanger length. In periods of high exhaust heat input, extended periods of super-heat are achieved, producing full (> 10 kW) turbine power. As heat input falls and superheat is lost, mass flow rate to the turbine is reduced, cutting output power (as a function of dryness fraction).

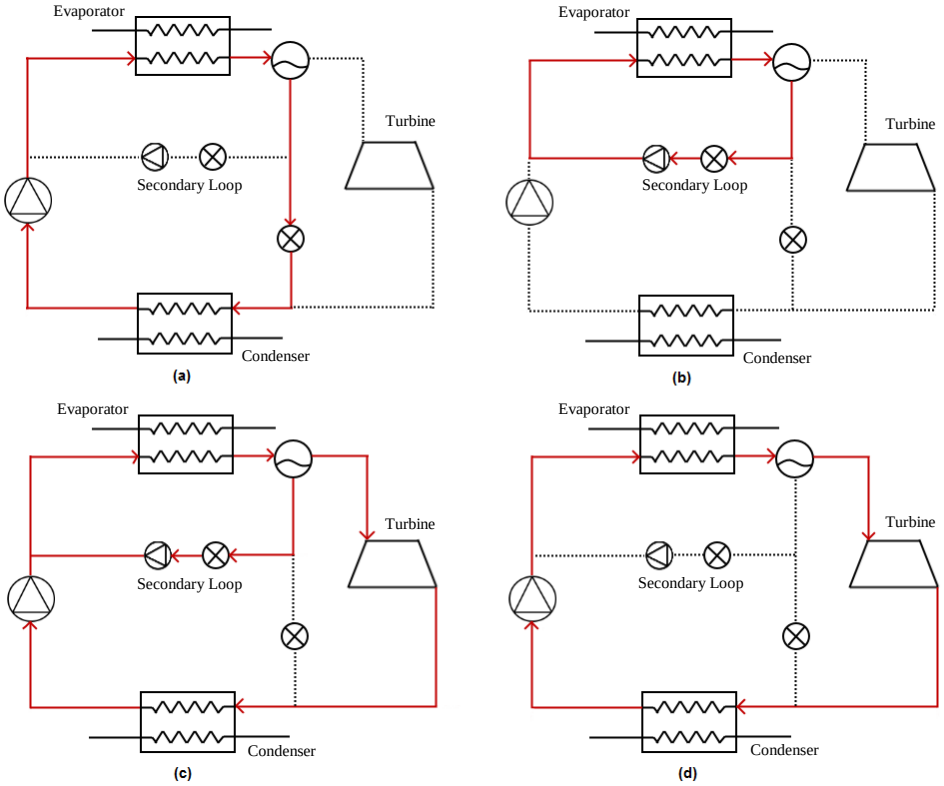

Figure 2: Flow paths are indicated in red for (a) warm-up, (b) sub-cooled, (c) boiling, and (d) super-heated

Table 3: Summary of duty cycles (DieselNet, 2015) used for transient thermodynamic ORC simulations

Duty Cycle	Originator	Length (s)	Focus
Constant-Speed, Variable-Load (CSVL)	US EPA	1200	Constant-speed engines; included here as a surrogate for off-road applications such as hydraulic excavators.
European Transient Cycle (ETC)	EU	1800	On-road; transient test cycle for truck and bus engines, used in part for heavy-duty engine emission certification.
Non-road Transient Cycle (NRTC)	US EPA/EU	1238	Off-road; transient engine dynamometer cycle for mobile off-road engines, for engine emission certification in the USA, EU and elsewhere.
World Harmonized Transient Cycle (WHTC)	UN ECE	1800	On-road; transient engine dynamometer cycle for heavy-duty engines, for engine emission certification worldwide.

Due to recirculation of saturated liquid back to the heat exchanger inlet, there is a deviation from expected behavior at high mass flow rates. In non-recirculating cycles, a sharp drop-off in average power is expected, as the exhaust flow no longer provides sufficient enthalpy to vaporize an increasing mass of fluid – a point will therefore be reached where zero power will be produced. In a recirculating cycle, it can be seen that as mass flow rate is increased, an increased proportion of saturated liquid will be produced, but this is recirculated to increase the heat exchanger inlet enthalpy. So, at large mass flow rates, no additional work will be extracted from the cycle, but rather than decreasing to zero, a minimum net power will be reached. This phenomenon is seen in Figure 5.

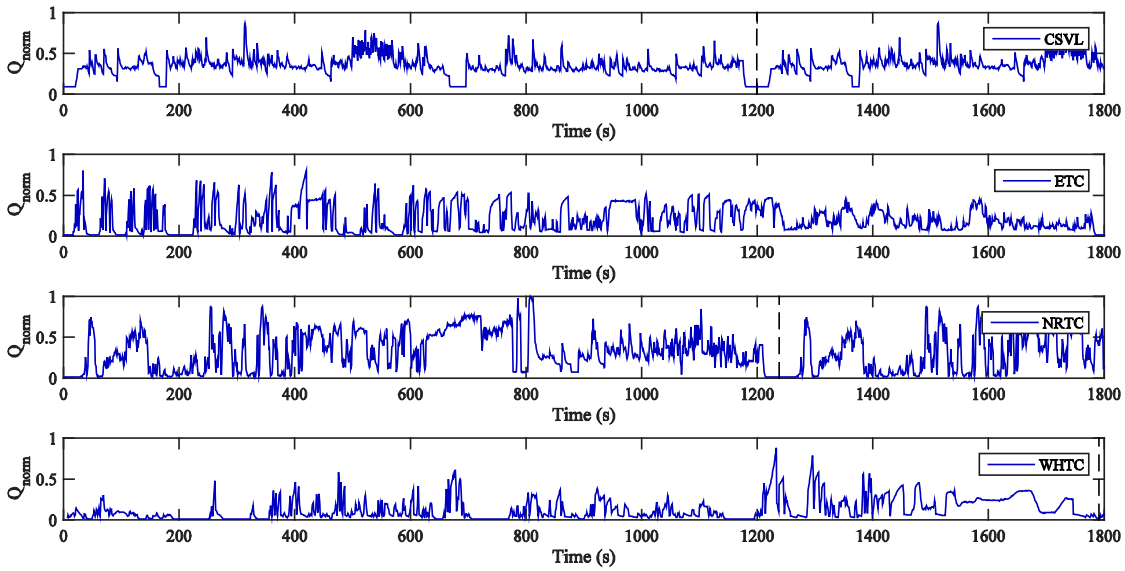

Figure 3: Time histories of normalized heat power, Q_{norm}, input into the ORC simulation for each duty cycle under examination (a broken vertical line denotes cycle repetition)

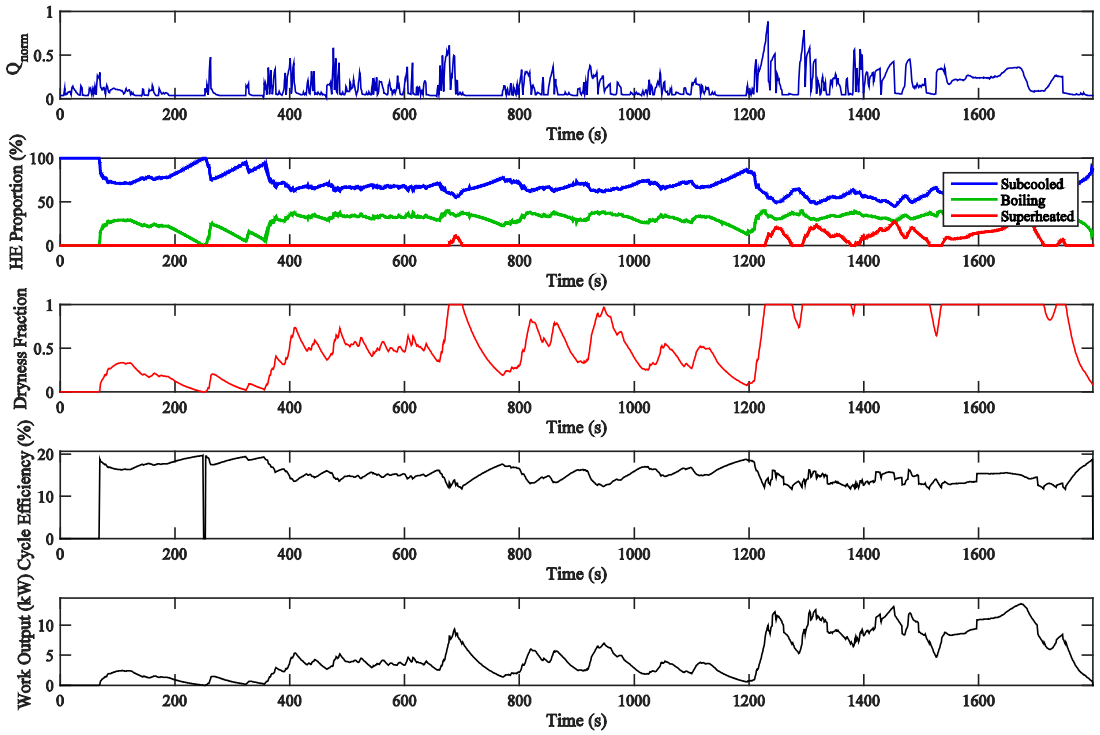

Figure 4: Key properties across a sample duty cycle (WHTC, 0.25 kg/s ORC mass flow rate). From top to bottom: normalized heat power (Q_{norm}); proportion of sub-cooled, boiling and superheated states ("HE Proportion"); dryness fraction; cycle efficiency; and work output

To illustrate the range of thermodynamic states encountered at the heat exchanger exit during a simulated duty cycle, Figure 6 presents two duty cycles (WHTC and CSVL) laid out on the T-S plane, superimposed on the R245fa saturation curve. The color map for each describes the relative proportion of time spent at each position on the 2400 kPa isobar. We may observe that the degree of variation across both duty cycles is very large – whilst in both cases the most time is spent under the saturation curve, there are extended periods of significant deviation from the optimal condition (on the saturated vapor line providing 100% mass flow to the turbine with no excess heat input). Secondly it

can be seen that the effectiveness of a heat exchanger sizing is highly dependent upon the nature of the heat source – whilst one cycle provides significant periods of super-heat (CSVL), another can fail to input sufficient power to fully vaporize the ORC working fluid.

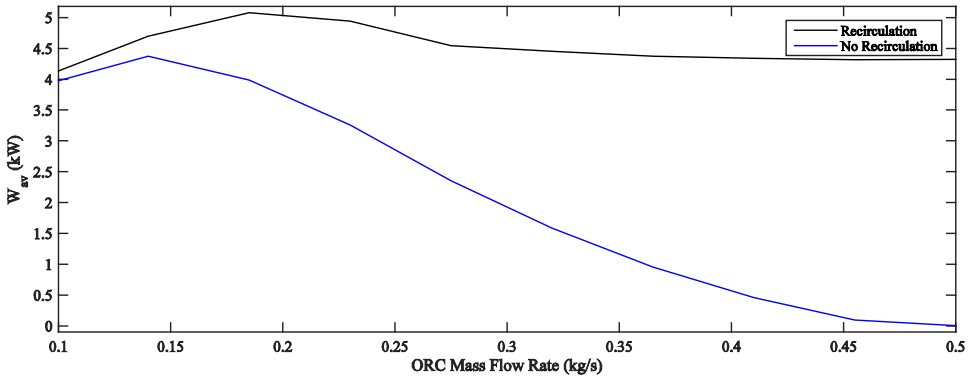

Figure 5: Sat. liquid recirculation raises average power output by increasing heat exchanger inlet enthalpy

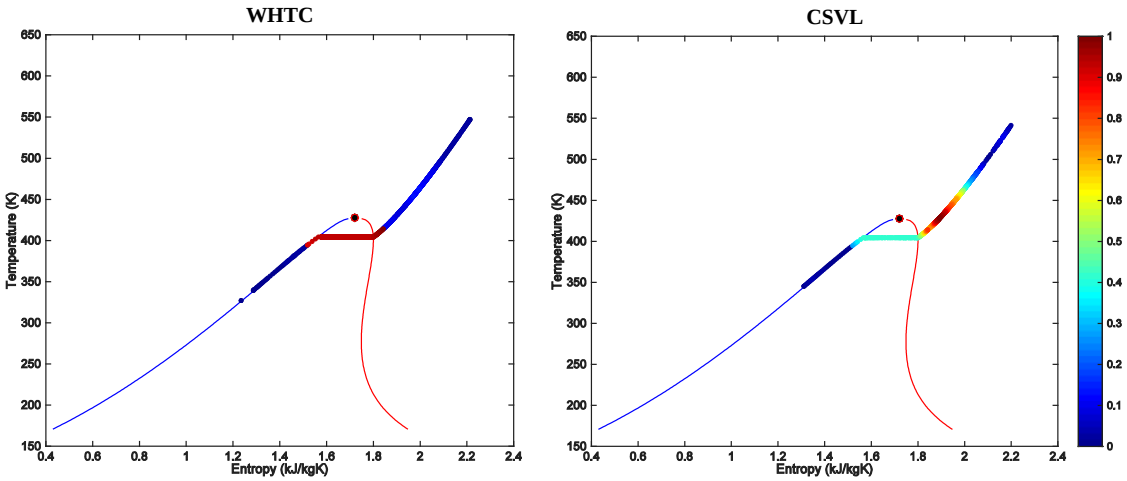

Figure 6: Range occupied in T-S plane for WHTC and CSVL duty cycles, with identical heat exchanger sizing and ORC mass flow rate set-points. Color map indicates fraction of time spent at each state

3.2. ORC Mass Flow Rate Variation

The primary figure of merit to maximize is the time-averaged power output across the entire duty cycle, which gives a pathway to quantifying potential fuel savings. ORC mass flow rate was set at the heat exchanger and in periods of saturated liquid recirculation from the heat exchanger outlet, the condenser mass flow was adjusted to meet this set-point. Ten simulations were conducted across each curve, as presented in Figure 7. Solutions that exceeded the R245fa maximum temperature of 300°C (where it would be stable for 100 hours (Angelino and Invernizzi, 2003)) were discarded, shown by the grey regions in Figures 7 and 8. Figure 7 shows a large difference between the average power output in each duty cycle. The CSVL cycle generates the highest output (9 kW), confirming the strong dependency between available exhaust energy and ORC system output. Sensitivity to heat exchanger size was quite modest, with less than 10% difference between designs. This is due to low exhaust-side convective heat transfer coefficients limiting the rate of heat transfer, irrespective of ORC pipe sizing.

3.3. Normalized ORC Power Recovery

To analyze the relative benefits of different duty cycles, each plot was normalized against the mean engine power, derived from temperature and mass flow rate traces. This gives a prediction of Exhaust Power Recovery (EPR), the time-averaged cycle efficiency over an entire transient duty cycle (Figure 8). It compares the power extracted to the theoretical maximum power available in the exhaust flow.

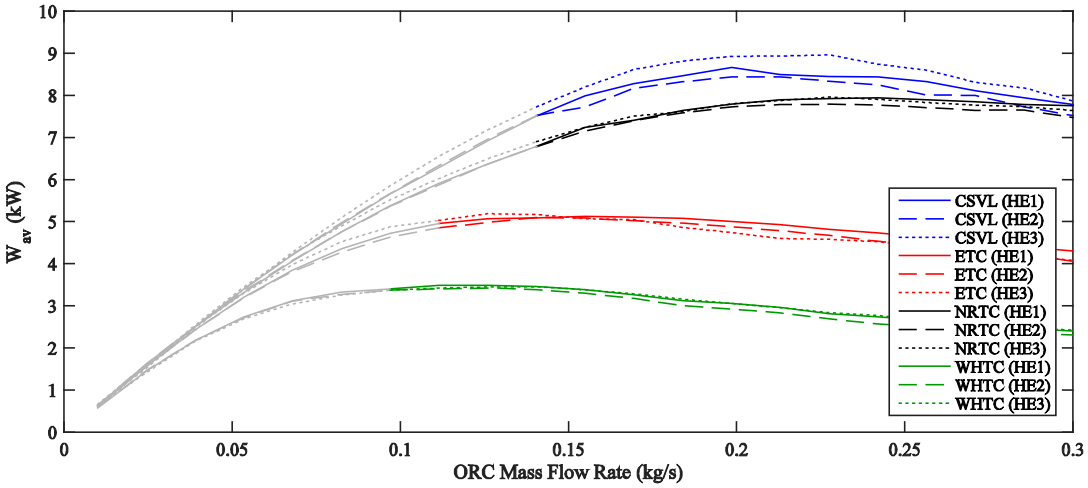

Figure 7: Cycle-averaged power output across each simulated duty cycle. Grey regions represent scenarios exceeding the maximum working fluid temperature.

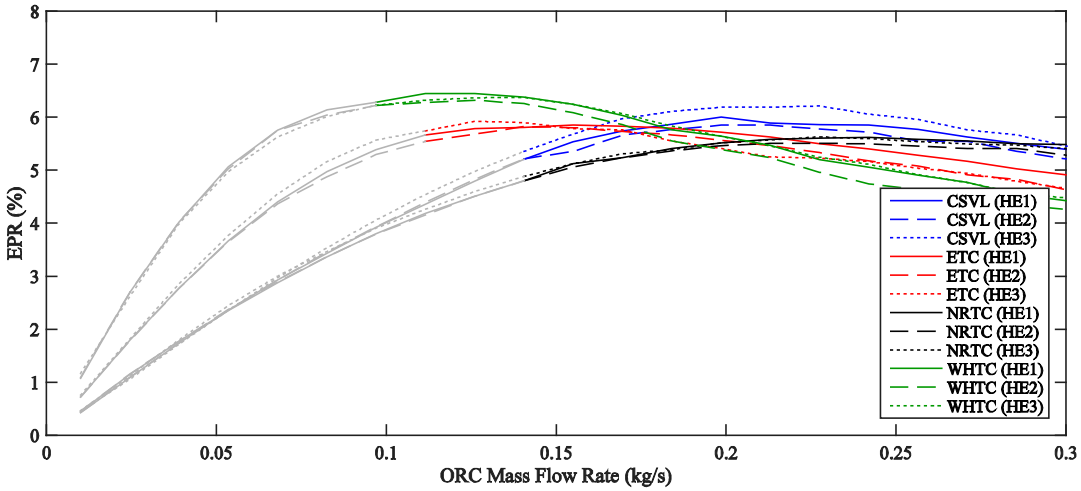

Figure 8: Exhaust Power Recovery (EPR) percentage for each duty cycle. Grey regions represent scenarios exceeding the maximum working fluid temperature.

Figure 8 shows that the peak values of Exhaust Power Recovery are at about the same level across all four duty cycles, with the highest (6.5%) being achieved by the low-power WHTC cycle. This is due to recirculation within the ORC system – this provides a pathway for fluid to be recirculated back to the heat exchanger inlet, allowing duty cycles which operate primarily at part-load to achieve increased efficiency. This is compounded by part-load operation increasing the proportion of boiling flow within the evaporator and therefore allowing increased heat exchanger effectiveness. While there is strong correlation between the available exhaust power and the level of ORC system output, it is also a relatively flat trend. Being taken from the point of exhaust entry to the ORC evaporator, this guarantees that as a given engine moves towards heavier duty cycles (and increased exhaust power ratings), ORC power output scales accordingly. A similar relationship may be valid across engine size, making mobile ORC systems promising for large heavy-duty diesel engines. With a key limitation on these applications being the ability to design turbomachinery to deliver acceptable isentropic efficiency at low power ratings, this scaling suggests that larger diesel engines stand to be the most promising candidates for initial mobile ORC system development.

4. CONCLUSIONS

This paper has detailed the development of a transient heat exchanger model based upon the NTU-effectiveness method, incorporating multiple operating states and correlations to accurately model

mobile ORC operation and start-up effects. A selection of reference transient duty cycles were taken as inputs to an engine simulation, providing mass flow and temperature boundary conditions to the ORC model, allowing insight into the transient cycle characteristics. For a fixed heat exchanger size, working fluid and ORC mass flow rate, different duty cycles were seen to produce a large variation in thermodynamic conditions at the evaporator outlet, along with the average power generated across a single duty cycle. Variation was such that a high-load CSVL cycle produced peak average power of 9.0 kW from start-up, whilst an on-highway WHTC only delivered 3.2 kW. Results were normalized against the theoretical exhaust power for each cycle, revealing a very narrow band (5.5-6.2%) of peak exhaust energy recovery across all duty cycles, suggesting a close to linear scaling of ORC system output with duty cycle output and engine sizing. The choice of vehicle/application is therefore primarily constrained by the ability to design acceptable low-power turbomachinery. A prediction is therefore made that vehicles running heavy duty cycles with high residual exhaust power have the potential to benefit the most from mobile ORC systems.

NOMENCLATURE

C	heat capacity	(kW K^{-1})
E	enhancement factor	(–)
f	friction factor	(–)
HE	heat exchanger	
h	heat transfer coefficient	(W m^{-2} K^{-1})
Nu	Nusselt number	(–)
ORC	organic Rankine cycle	
Pr	Prandtl number	(–)
Q	power (heat)	(kW)
Re	Reynolds number	(–)
S	suppression factor	(–)
T	temperature	(K)
t	time	(s)
W	power (work)	(kW)

Greek letters

τ	time constant	(s)

Subscripts

0	current value
av	time-averaged value
casing	referring to the heat exchanger metal casing
D	referred to diameter
exh	exhaust gas
inf	steady-state value
l	liquid
norm	normalized value
orc	ORC working fluid
pipe	referring to the heat exchanger metal piping
pool	pool boiling
TP	two-phase

REFERENCES

Aly, A.E., 1988, Diesel engine waste-heat power cycle, *Applied Energy*, Vol. 29, p. 179-189.

Angelino, G., Invernizzi, C., 2003, Experimental investigation on the thermal stability of some new zero ODP refrigerants, *Int. J. Refrigeration*, Vol. 26, p. 51-58.

Auto Council, 2011, Commercial Vehicle & Off-Highway Low Carbon Technology Roadmap.

Badr, O., Probert, S.D., O'Callaghan, P.W., 1985, Selecting a working fluid for a Rankine-cycle engine, *Applied Energy*, Vol. 21, p. 1-42.

Costall, A.W., Gonzalez Hernandez, A., Newton, P.J., Martinez-Botas, R.F., 2015, Design methodology for radial turbo expanders in mobile organic Rankine cycle applications, *Applied Energy*, Article in Press, http://dx.doi.org/10.1016/j.apenergy.2015.02.072.

DiNanno, L.R., DiBella, F.A., Koplow, M.D., 1983, A*n RC-1 organic Rankine bottoming cycle for an adiabatic diesel engine*, NASA, DOE/NASA/0302-1.

DieselNet, 2015, Emission Test Cycles. Worldwide Engine and Vehicle Test Cycles, URL: https://www.dieselnet.com/standards/cycles, Accessed: 2015-03-20.

Endo, T., Kawajiri, S., Kojima, Y., Takahashi, K., Baba, T., Ibaraki, S., Takahashi, T., Shinohara, M., 2007, Study on Maximizing Exergy in Automotive Engines, in: *Proceedings of the SAE 2007 World Congress and Exhibition*, SAE Technical Paper 2007-01-0257.

EPA, 2011, Greenhouse Gas Emissions Standards and Fuel Efficiency Standards for Medium- and Heavy-Duty Engines and Vehicles, *Federal Register*, Vol. 76, No. 179, p. 57106-57513.

Greszler, A., 2012, View from the Bridge – Commercial Vehicle Perspective, in: *Proceedings of the 18th Directions in Engine-Efficiency and Emissions Research (DEER) Conference*.

Gungor, K.E., Winterton, R.H.S., 1986, A general correlation for flow boiling in tubes and annuli, *Int. J. Heat Mass Transfer*, Vol. 29, No. 3, p. 351-358.

Hedbom, A., 2007, *SCANIA DC12 01 Euro 3 Engine. Emission Measurements for VTI and COST 346*, Report N52A-2005, Swedish National Road and Transport Research Institute (VTI).

Horst, T.A., Tegethoff, W., Eilts, P., Koehler, J., 2014, Prediction of dynamic Rankine Cycle waste heat recovery performance and fuel saving potential in passenger car applications considering interactions with vehicles' energy management, *Energy Conversion and Management*, Vol. 78, p. 438-451.

Howey, D., North R., Martinez-Botas, R., 2010, *Road transport technology and climate change mitigation*, Grantham Institute for Climate Change Briefing paper No 2.

Incropera, F.P., DeWitt, D.P., Bergman, L., Lavine, A.S., 2006, *Fundamentals of Heat and Mass Transfer*, John Wiley & Sons, 6th Edition.

Kakaç, S., 1991, *Boilers, Evaporators and Condensers*, John Wiley & Sons, 1st Edition.

Katsanos, C.O., Hountalas, D.T., Pariotis, E.G., 2012, Thermodynamic analysis of a Rankine cycle applied on a diesel truck engine using steam and organic medium, *Energy Conversion and Management*, Vol. 60, p. 68-76.

Koeberlein, D., 2013, *Technology and System Level Demonstration of Highly Efficient and Clean, Diesel Powered Class 8 Trucks*, DOE Hydrogen and Fuel Cells Program, and Vehicle Technologies Program Annual Merit Review and Peer Evaluation.

Lachi, M., el Wakil, N., Padet, J., 1997, The time constant of double pipe and one pass shell-and-tube heat exchangers in the case of varying fluid flow rates, *Int. J. Heat Mass Transfer*, Vol. 40, No. 9, p. 2067-2079.

Leising, C., Purohit, G., DeGrey, S., and Finegold, J., 1978, Waste Heat Recovery in Truck Engines, SAE Technical Paper 780686.

Macchi, E., Perdichizzi, A., 1981, Efficiency Prediction for Axial-Flow Turbines Operating with Nonconventional Fluids, *ASME Journal of Engineering for Power*, Vol. 103, p. 718-724,

Peralez, J., Tona, P., Sciarretta, A., Dufour, P., Nadri, M., 2014, Optimal Control of a Vehicular Organic Rankine Cycle via Dynamic Programming with Adaptive Discretization Grid, in: *Proceedings of the IFAC 19th World Congress*, p. 5671-5678.

Quoilin, S., Declaye, S., Lemort, V., 2010, Expansion Machine and Fluid Selection for the Organic Rankine Cycle, *7th Int. Conf. on Heat Transfer, Fluid Mechanics and Thermodynamics*, p. 1-7.

Quoilin, S., Van Den Broek, M., Declaye, S., Dewallef, P., Lemort, V., 2013, Techno-economic survey of Organic Rankine Cycle (ORC) systems. *Renewable and Sustainable Energy Reviews*, Vol. 22, p. 168-186.

Sprouse, C. III and Depcik, C., 2013, Review of organic Rankine cycles for internal combustion engine exhaust waste heat recovery, *Applied Thermal Eng.*, Vol. 51, Nos. 1-2, p. 711-722.

Uusitalo, A., Larjola, J., and Turunen-Saaresti, T., 2011, Background and summary of commercial ORC, in: Proceedings *of ORC 2011: First International Seminar on ORC Power Systems*.